



Radiation hydrodynamics simulations of brown dwarf atmospheres with CO5BOLD

B. Freytag, F. Allard, and D. Homeier

Centre de Recherche Astrophysique de Lyon, UMR 5574: CNRS, Université de Lyon, École Normale Supérieure de Lyon, 46 allée d'Italie, F-69364 Lyon Cedex 07, France

Abstract. The interplay of radiative and hydrodynamic processes governs the stratified atmospheres of cool stars and substellar objects, with the underlying convection zone playing an important role. At sufficiently low temperatures, matter can condense into dust grains, whose formation, growths, destruction, and gravitational settling critically depend on the thermal structure of the atmosphere. Equally important are horizontal and vertical mixing and transport of material, that can compensate the rain-out of dust, induced on small scales by convective motions, overshoot, gravity waves, and turbulence, but also on larger scales by a global wind system strongly influenced by the rapid rotation of a typical brown dwarf. Local and first simple global radiation-hydrodynamics simulations of cool objects with the CO5BOLD code are presented.

Key words. Stars: atmospheres – Numerical methods: hydrodynamics

1. Introduction

The radiation-magneto-hydrodynamics code CO5BOLD is constructed to account for the conditions in the atmospheres of cool stars and substellar objects, as well as the convective surface layers below (Freytag et al. 2012). Separate modules solve either the hydrodynamics equations or the magneto-hydrodynamics equations. Both account for ionization effects, gravity, and compressibility. There are two different geometrical setups: the one for local “box-in-a-star” models of a small patch of the stellar surface accounts for horizontally periodic boundary conditions (e.g., Steffen et al. 2009; Ludwig & Kučinskas 2012). The other one is intended for performing global “star-in-a-box” simulations of (essentially) the entire stellar envelope (Freytag

et al. 2002; Freytag & Höfner 2008). Both account for non-local radiation-transport and frequency-dependent opacities via an opacity-binning scheme. Various optional modules account for molecule or dust formation (e.g., Freytag & Höfner 2008; Freytag et al. 2010).

The solar model presented in Fig. 1 shows the usual granular pattern of solar surface convection with bright granules with hot upward flowing material surrounded by dark intergranular lanes that representing cool downdrafts. The latter are the site of largest convective velocities (just below the visible surface), with large amount of shear, turbulence, and vortices (visible as small bright dots within the dark intergranular lanes, see e.g., Wedemeyer-Böhm et al. 2012). The flow field is not restricted to the convectively stable layers below the surface but shows up as overshoot (Freytag et al.

Send offprint requests to: B. Freytag

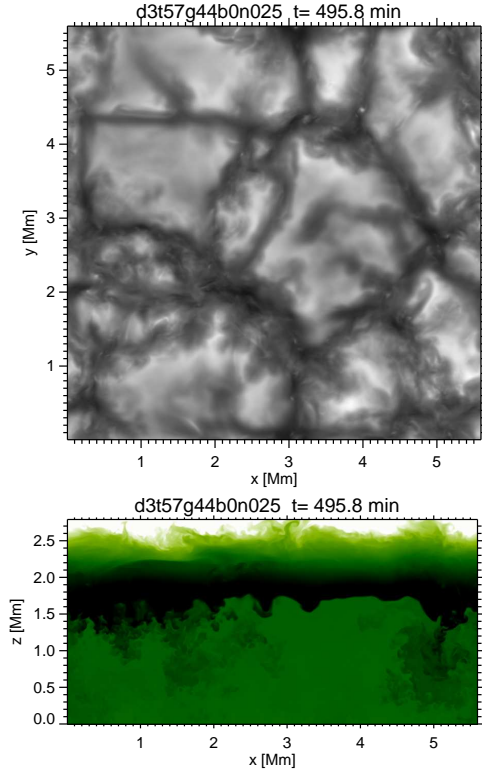


Fig. 1. Plots of emergent grey surface intensity (top) and entropy (bottom) of a 3D solar model with a high resolution of $800^2 \times 400$ grid points.

1996) and (predominantly pressure-) waves in the lower photosphere. These waves turn into shocks in the upper part of the photosphere and can contribute to the formation of a chromosphere (Wedemeyer et al. 2004).

2. From the Sun to brown dwarfs

Figure 2 shows the mean entropy and rms vertical velocity (averaged horizontally and over time) for an effective-temperature sequence of radiation-hydrodynamics (RHD) models along the main sequence. Above the entropy plateau in the deeper layers sit the (more or less pronounced) superadiabatic layers. The entropy minimum marks the top of the convectively unstable layers. Above sits the convectively stable photosphere.

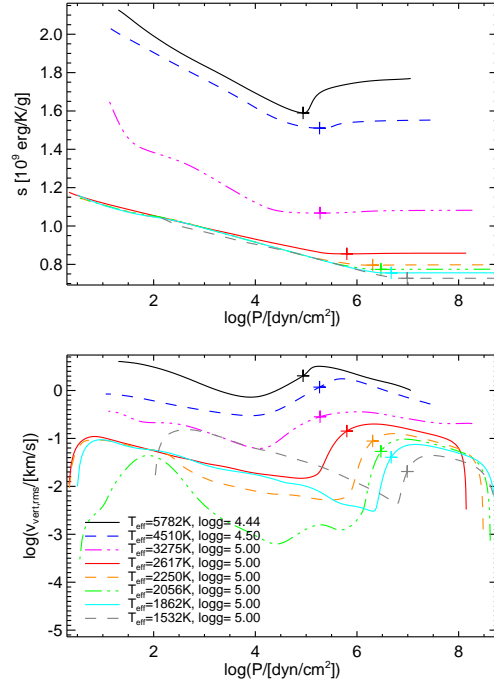


Fig. 2. Entropy and rms vertical velocity for selected (sub)stellar models. The plus signs indicate the position of the entropy minimum (the top of the convectively unstable layers). The curves follow the order in the legend from top to bottom.

With decreasing effective temperature, the value of the entropy plateau decreases. More dramatic is the shrinking (in entropy amplitude and geometrical extension) of the superadiabatic layers. This change is also visible in the rms vertical velocity: the convective velocities – and also the corresponding Mach numbers – decrease and the decline at the top of the convection zone becomes steeper. Nevertheless, contrary to predictions of the mixing-length theory, the velocities do not drop to zero but decay smoothly (Freytag et al. 1996), reach a minimum, and increase again mostly due to pressure waves in the hotter models and predominantly gravity waves in the coolest models. Below $T_{\text{eff}} \approx 2000$ K, convection within the photospheric dust cloud layers (and waves generated by it) contribute to the velocity field.

With decreasing effective temperature, the radiative relaxation time scales increase. A ma-

terial parcel “hitting” the top of the unstable layers of a brown dwarf convection zone from below can hardly penetrate into the stable layers above: the braking buoyance force is too strong. The velocity scale height of vertical overshoot – the region in which the upflows are turned horizontally – is small, giving rise to the production of gravity waves, which also have a predominantly horizontal component.

The change in properties of the atmospheres and convection zones along the main sequence has a number of consequences for the requirements on RHD simulations:

While the convective flow in solar granules reaches or exceeds Mach numbers of one and the shocks in the upper photosphere and the chromosphere typically has supersonic speeds (Wedemeyer et al. 2004), the convective flows in brown dwarfs have only small Mach numbers (Freytag et al. 2010) and are nearly incompressible. Only the predominantly horizontal flows in the top layers of brown-dwarf models reach Mach numbers of one.

The well-mixed atmospheres of solar-like stars can be described in good approximation with two state variables per grid cell, e.g. density ρ and internal energy e_i . Further quantities (temperature, pressure, opacities) are derived during the RHD simulations by a lookup in tables (for some exceptions see e.g., Wedemeyer-Böhm et al. 2005; Leenaarts & Wedemeyer-Böhm 2006). However, the properties of dust grains depend on their history – values of temperature, gas density, partial pressures of molecules, and concentration of other dust species over time. Consequently, dust has to be described with additional density arrays $\rho_{\text{dust},i}$. The modelling of the evolution of dust has to take into account its advection but also nucleation, growth, and evaporation, for different grain sizes and compositions. This is a formidable task and so far only simple dust models have been implemented in CO5BOLD: a 4-moment model for carbon-rich dust in AGB stars (Freytag & Höfner 2008), a 2-bin model with “easy” nucleation for forsterite in brown dwarfs (Freytag et al. 2010), and multi-size-bin model with detailed nucleation for forsterite in brown dwarfs.

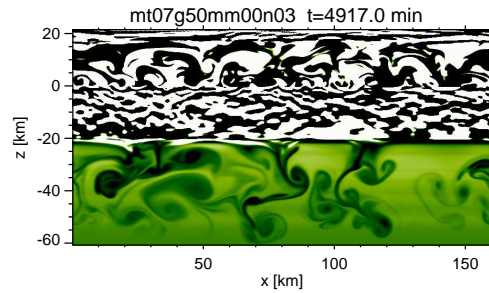


Fig. 3. Entropy fluctuations of a 700 K 2D brown dwarf model.

Solar granulation looks pretty much the same everywhere on the surface – sufficiently far away from the relatively small magnetic sunspots – and allows to represent the entire surface by a rather small patch that easily fits into the computational box. In contrast, observed photometric variability of brown dwarfs particularly near the L-T transition give strong hints to the possibility of large-fluctuations in the cloud properties. Several variable brown dwarfs are now known, two of them with very large variability amplitudes of 5-25 % in the near-infrared (Artigau et al. 2009; Radigan et al. 2012). Two highly variable early T dwarfs show evidence for a mixture of thin and thick clouds, rather than clouds with deep holes (Apai et al. 2013). A T6 dwarf is also variable and we found a surprising correlation between the light curve phase and pressure probed at a given wavelength. This indicates heterogeneous atmospheric structure in three dimensions (Buenzli et al. 2012).

Figure 3 shows the entropy fluctuations of a 2D model of the surface layers a 700 K brown dwarf, extending the sequence by Freytag et al. (2010) to lower effective temperatures with a new less diffusive version of CO5BOLD. The effective temperature is taken from the Phoenix atmosphere used to construct the start model. The actual effective temperature is much lower because of the enormous vertical extent of the dust cloud layers – likely due to the restriction to too small dust grains.

The dark inverted mushroom in the gas convection zone (below $z \approx -20$ km) show cool sinking material. The entropy fluctuations in

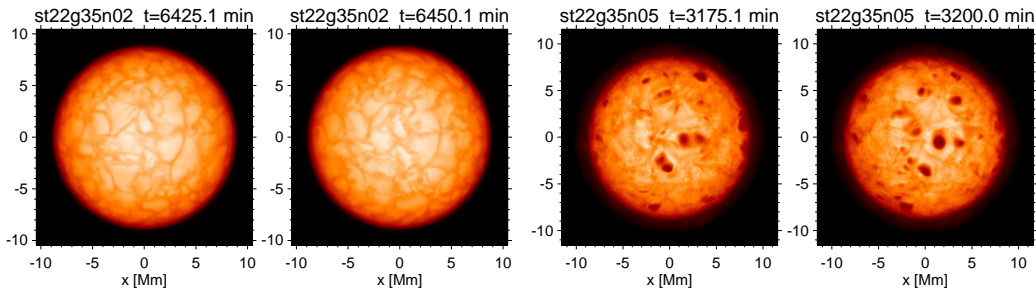


Fig. 4. Two intensity snapshots of a dust-free global brown dwarf toy model, about 25 min apart.

the photosphere above are much larger and therefore “overexposed” in this plot. Still, one can distinguish the dust convection zone with overturning flows ($-1 < z < 16$ km) from the regions filled by horizontally elongated gravity waves just below and above. If the dust clouds become so thick that they can hinder the radiative flux from escaping the develop internal convective flows very effectively mix material, a mechanism that depends sensitively on the properties of the employed dust model. Convective overshoot of the gas convection zone can only affect dust species that can form at the relatively high temperatures close to the convective layers. In contrast, gravity waves seem to occur everywhere, but there essentially reversible motion provides only small amounts of mixing (Freytag et al. 2010).

A parametrized description of the mixing based in CO5BOLD simulation was put into the Phoenix code and is part of the current Phoenix model generation (Allard et al. 2011, 2012). Figure 4 of Allard et al. (2011) and Figure 5 of Allard et al. (2013) show an effective-temperature sequence of intensity maps of local 3D RHD models of dusty brown dwarfs. With decreasing T_{eff} and increasing thickness of the clouds the underlying low-contrast granules become completely invisible. Instead, high-contrast small-scale features produced within the cloud layers dominate.

Figure 3 of Allard et al. (2013) shows the emergent intensity of a global 3D toy model of an M dwarf: While the surface properties (T_{eff} , $\log g$, and therefore pressure scale height and granule size) are realistic, the stellar radius was

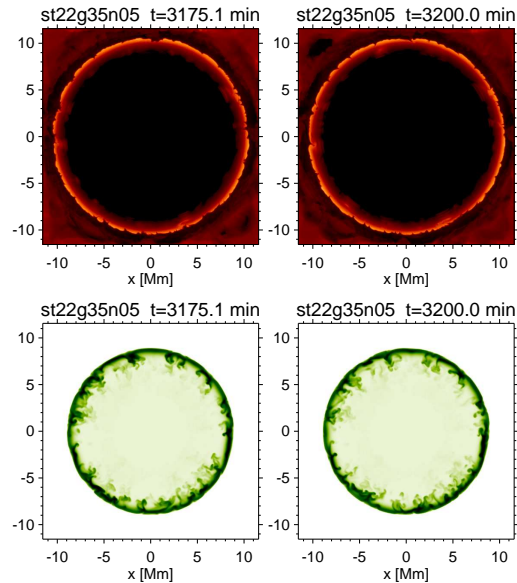


Fig. 5. Two intensity snapshots of a dusty global brown dwarf toy model, about 25 min apart (top panels). Below slices showing the dust concentration (middle) and the entropy (bottom).

drastically reduced so that only a small number of granules cover the entire surface. Such models of rotating M dwarfs are being used to determine the effect of rotation on the convective efficiency. A similar setup is used for the non-rotating models in Fig. 5 to study the occurrence of large-scale structure in the dust layers of brown dwarfs.

The very small convective cells in the thin dust layer have rather low contrast. The visible dark patches have roughly the scale of the underlying granules and are produced by occasionally occurring strong overshooting mo-

tions reaching up from the gas convection zone into the cloud layers.

While it is currently extremely difficult to cover the small-scale atmospheric features in a global model of a brown dwarf with a realistic radius, the presented toy models should be capable in the near future to represent qualitatively the interaction of small-scale and “global” structures.

3. Discussion and conclusions

Local radiation-hydrodynamics models of the dusty atmospheres and the underlying top layers of the convection zone of brown dwarfs have demonstrated that overshoot, gravity waves, and convection with the dust-clouds contribute in different layers to various degrees to the mixing and transport of material, that can counteract the rainout of dust grains. The clouds can show fast (\approx minutes) small-scale (\approx 100 km) high-contrast intensity fluctuations.

Several feedback mechanisms can be seen at work in the simulations, e.g. a positive one: Sufficiently (optically) thick dust clouds can lead to such a temperature gradient within the cloud layers that these become convectively unstable. The resulting convective motions effectively mix material and sustain the clouds. On the other hand can the presence of dust grains suppress the nucleation process, i.e. the formation of new small grains, by capturing all available potential dust constituents. That leads to growth in the average grain size, because grains might still evaporate at the hot bottom layers of clouds. Larger grains mean more efficient gravitational settling and as a result a reduction of the cloud thickness – a negative feedback mechanism. The interplay of such mechanism might play a role in producing large-scale variations in the cloud properties.

Future work will on the one hand concentrate on improved dust microphysics, that can be well studied by small local models as done so far. On the other hand, larger local and “global toy” models will be used to investigate the occurrence of large-scale dust inhomogeneities produced by instabilities in the dust physics themselves and/or by rotation. These 2D and 3D time-dependent CO5BOLD models will be complemented as before with 1D stationary equilibrium Phoenix models, that can

account for a much more complex radiation transport and chemical network as CO5BOLD.

Acknowledgements. The project was financed by the Agence Nationale de la Recherche (ANR), and the Programme National de Physique Stellaire (PNPS) of the Centre National de Recherche Scientifique (CNRS). The computations were performed at the Pôle Scientifique de Modélisation Numérique (PSMN) at the École Normale Supérieure (ENS) in Lyon.

References

- Allard, F., Homeier, D., & Freytag, B. 2011, in 16th Cambridge Workshop on Cool Stars, Stellar Systems, and the Sun, eds. C.M. Johns-Krull, M.K. Browning, & A.A. West, (ASP, San Francisco), ASP Conf. Ser., 448, 91
- Allard, F., Homeier, D., & Freytag, B. 2012, Royal Society of London Philosophical Transactions Series A, 370, 2765
- Allard, F., et al. 2013, Mem. SAI, Suppl. 24, 128
- Apai, D., et al. 2013, ApJ, 768, 121
- Artigau, É., Bouchard, S., Doyon, R., & Lafrenière, D. 2009, ApJ, 701, 1534
- Buenzli, E., Apai, D., Morley, C. V., et al. 2012, ApJ, 760, L31
- Freytag, B., & Höfner, S. 2008, A&A, 483, 571
- Freytag, B., Ludwig, H. G., & Steffen, M. 1996, A&A, 313, 497
- Freytag, B., Steffen, M., & Dorch, B. 2002, Astron. Nachr., 323, 213
- Freytag, B., Allard, F., Ludwig, H.-G., et al. 2010, A&A, 513, A19
- Freytag, B., Steffen, M., Ludwig, H. G., et al. 2012, J.Comp.Phys., 231, 919
- Leenaarts, J., & Wedemeyer-Böhm, S. 2006, A&A, 460, 301
- Ludwig, H. G., & Kučinskas, A. 2012, A&A, 547, A118
- Radigan, J., Jayawardhana, R., Lafrenière, D., et al. 2012, ApJ, 750, 105
- Steffen, M., Ludwig, H. G., & Caffau, E. 2009, MmSAI, 80, 731
- Wedemeyer, S., Freytag, B., Steffen, M., et al. 2004, A&A, 414, 1121
- Wedemeyer-Böhm, S., Kamp, I., Bruls, J., & Freytag, B. 2005, A&A, 438, 1043
- Wedemeyer-Böhm, S., Scullion, E., Steiner, O., et al. 2012, Nature, 486, 505